Journal for ImmunoTherapy of Cancer

Molecular underpinnings of exceptional response in primary malignant melanoma of the esophagus to anti-PD-1 monotherapy

Jie Dai ,[1] Xue Bai ,[1] Xuan Gao,[2,3] Lirui Tang,[1] Yu Chen,[4] Linzi Sun,[1] Xiaoting Wei,[1] Caili Li,[1] Zhonghui Qi,[1] Yan Kong,[1] Chuanliang Cui ,[1] Zhihong Chi,[1] Xinan Sheng ,[5] Zelong Xu,[6] Bin Lian ,[1] Siming Li,[1] Xieqiao Yan,[5] Bixia Tang ,[5] Li Zhou ,[5] Xuan Wang,[1] Xuefeng Xia,[6] Jun Guo,[1,5] Lili Mao,[1] Lu Si[1]

To cite: Dai J, Bai X, Gao X, *et al*. Molecular underpinnings of exceptional response in primary malignant melanoma of the esophagus to anti-PD-1 monotherapy. *Journal for ImmunoTherapy of Cancer* 2023;**11**:e005937. doi:10.1136/jitc-2022-005937

► Additional supplemental material is published online only. To view, please visit the journal online (http://dx.doi.org/10.1136/jitc-2022-005937).

JD, XB and XG contributed equally.

Accepted 07 December 2022

Check for updates

© Author(s) (or their employer(s)) 2023. Re-use permitted under CC BY-NC. No commercial re-use. See rights and permissions. Published by BMJ.

For numbered affiliations see end of article.

Correspondence to
Dr Lu Si; silu15_silu@126.com

Dr Lili Mao; yunzhongmanbu7848@163.com

ABSTRACT

Background Accumulating data suggest that mucosal melanoma, well known for its poor response to immune checkpoint blockade (ICB) and abysmal prognosis, is a heterogeneous subtype of melanoma with distinct genomic and clinical characteristics between different anatomic locations of the primary lesions. Primary malignant melanoma of the esophagus (PMME) is a rare, highly aggressive disease with a poorer prognosis compared with that of non-esophageal mucosal melanoma (NEMM). In this study, we retrospectively analyzed the efficacy of anti-programmed death (PD)-1 in patients with PMME and explored its molecular basis.

Methods The response and survival of patients with PMME and NEMM under anti-PD-1 monotherapy were retrospectively analyzed. To explore the molecular mechanisms of the difference in therapeutic efficacy between PMME and NEMM, we performed genomic analysis, bulk RNA sequencing, and multiplex immunohistochemistry staining.

Results We found that PMME (n=28) responded better to anti-PD-1 treatment than NEMM (n=64), with a significantly higher objective response rate (33.3% (95% CI 14.3% to 52.3%) vs 6.6% (95% CI 0.2% to 12.9%)) and disease control rate (74.1% (95% CI 56.4% to 91.7%) vs 37.7% (95% CI 25.2% to 50.2%)). Genomic sequencing analysis revealed that the genomic aberration landscape of PMME predominated in classical cancer driver genes, with approximately half of PMME cases harboring mutations in *BRAF*, *N/KRAS*, and *NF1*. In contrast, most NEMM cases were triple wild-type. Transcriptome analysis revealed that, compared with NEMM, PMME displayed more significant proliferation and inflammatory features with higher expression of genes related to antigen presentation and differentiation, and a less immunosuppressive signature with lower expression of inhibitory immune checkpoints and dedifferentiation-related genes. The multiplex immunohistochemical analysis also demonstrated higher $CD8^+$ T-cell infiltration in PMME than in NEMM.

Conclusions PMME is an outlier of mucosal melanoma showing a malicious phenotype but a particularly high response rate to ICB because of its distinct molecular characteristics. Patient stratification based on anatomic origin can facilitate clinical decision-making in patients with mucosal melanoma following the verification of our results in future prospective studies.

WHAT IS ALREADY KNOWN ON THIS TOPIC

⇒ Anti-PD-1 monotherapy has limited efficacy in mucosal melanoma. The incidence of primary malignant melanoma of the esophagus (PMME) is extremely low, and its survival is shorter than that of non-esophageal mucosal melanoma (NEMM).

⇒ The efficacy of anti-PD-1 monotherapy in PMME and the molecular characteristics and immune infiltration features of PMME remain unclear.

WHAT THIS STUDY ADDS

⇒ PMME exhibits a more favorable response to anti-PD-1 treatment than NEMM.

⇒ PMME shows more inflammatory features than NEMM.

⇒ PMME harbors more aberrations in canonical driver genes and exhibits greater proliferation than NEMM, resulting in more aggressive behavior.

HOW THIS STUDY MIGHT AFFECT RESEARCH, PRACTICE OR POLICY

⇒ This study provides preliminary data on the efficacy of anti-PD-1 monotherapy in PMME and indicates that PMME is a specific type of mucosal melanoma with a more proliferative molecular signature but responds better to anti-PD-1 treatment than NEMM.

BACKGROUND

Mucosal melanoma arises from the malignant transformation of melanocytes located at mucosal membranes. The incidence of mucosal melanoma is lower than that of cutaneous melanoma. The common sites of mucosal melanoma include the nasopharyngeal and oral, lower gastrointestinal, and

gynecological tissues, and the stage, nodal and distant metastases, distant metastases predilection sites, and overall survival (OS) are similar between different primary anatomic sites.[1] Therefore, mucosal melanoma was previously treated as a single histological subtype. Primary malignant melanoma of the esophagus (PMME) is a rare disease, which is more aggressive and has a poorer prognosis than non-esophageal mucosal melanoma (NEMM), and its etiology and pathogenesis are poorly understood. The median time to recurrence of patients with PMME who underwent surgery and median OS from diagnosis are 5.9–6 and 13.5–18.1 months, respectively. The 5-year survival rate of PMME is significantly lower than that of NEMM.[2–4]

Immune checkpoint blockade (ICB) is the main therapeutic approach for advanced melanoma and leads to improved clinical outcomes.[5] Numerous factors were reported to be associated with the response to ICB, such as $CD8^+$ T-cell infiltration, programmed death ligand (PD-L1) expression, tumor mutational burden (TMB), insertion/deletion (indel) burden, tumor neoantigen burden (TNB), human leukocyte antigen (HLA)-corrected TMB, antigen presentation, and mutation status of *JAK1/2*, *PTEN*.[6–10] However, the clinical benefits of ICB in mucosal melanoma are limited because of the lower TMB and tumor PD-L1 expression in this subtype.[11–13] The molecular characteristics and immune infiltration features of PMME remain unclear, and there is no standard treatment for patients with advanced PMME because of the lack of strong clinical evidence.

In this study, we retrospectively analyzed patients with mucosal melanoma who were treated with anti-PD-1 monotherapy in our center and compared its efficacy against PMME and NEMM. Genome and RNA sequencing as well as multiplex immunohistochemistry (mIHC) staining were performed and compared in retrospectively assembled samples from patients with either PMME or NEMM to characterize the genomic and transcriptomic landscape and tumor immune microenvironment.

MATERIALS AND METHODS

Patients

The data of patients with advanced mucosal melanoma treated with anti-PD-1 monotherapy (including pembrolizumab, toripalimab, and camrelizumab) between July 2015 and July 2022 (last follow-up in October 2022) within and outside of the clinical trial setting at Peking University Cancer Hospital were extracted and reviewed. Radiological evaluations were conducted either by treating physicians or independent radiologists as per Response Evaluation Criteria in Solid Tumors (V.1.1). The overall response rate (ORR) was defined as the proportion of patients who achieved a complete response (CR) or partial response (PR). The disease control rate (DCR) was defined as the proportion of patients who had stable disease or achieved a CR or PR. Progression-free survival (PFS) was defined as the time from the start of treatment to progression or last follow-up. OS was defined as the time from the start of treatment to death or last follow-up. Disease-free survival (DFS) was defined as the time from the surgery to the date of recurrence or metastases. For the molecular and cellular underpinning study, the primary tumor samples and matched peripheral blood samples were collected between December 2012 and January 2019.

DNA extraction and genomic sequencing

The genomic DNA from fresh frozen tumor tissue and matched normal samples was isolated using a DNeasy Blood & Tissue Kit (Qiagen, Hilden, Germany). From formalin-fixed paraffin-embedded (FFPE) samples, DNA was extracted using a Maxwell RSC DNA FFPE kit (Promega, Madison, Wisconsin, USA). A library was constructed using an NEBNext Ultra II DNA Kit (New England Biolabs, Ipswich, Massachusetts, USA) and sequenced on a HiSeq 3000 Sequencing platform (Illumina, San Diego, California, USA), with 100 bp paired-end reads.

Fastp was used to filter out low-quality and short reads and to trim the adapters from the raw reads to obtain clean reads. The clean reads were aligned to the GRCh37 assembly using Burrows-Wheeler Aligner. Binary files (BAM) were created using samtools. Somatic single-nucleotide variants and short indels were detected using GATK HaplotypeCaller (V.4.1.2.0) and Mutect2 (V.4.1.4.1) software. Somatic non-synonymous mutations per megabase of the panel region annotated by the Ensembl variant effect predictor were used in TMB analysis. Copy number variations (CNVs) were expressed as the ratio of the adjusted depth between tumor tissue DNA and germline DNA and were analyzed using FACETS with log2 ratio thresholds of 0.322 and −0.415 for gain and loss, respectively.

HLA genotyping and neoantigen identification

HLA genotyping was predicted by OptiType, an HLA genotyping algorithm based on integer linear programming that is capable of producing accurate four-digit HLA genotyping predictions from next-generation sequencing data by simultaneously selecting all minor and major HLA-I alleles. Loss of heterozygosity in HLA (HLA-LOH) was identified by the HLALOH repository, a computational tool that evaluates HLA loss using next-generation sequencing data and HLA genotyping. We used pVACseq software to predict major histocompatibility complex (MHC)-I class neoantigen based on missense, in-frame insertion, in-frame deletion, protein-altering, frameshift mutations, and HLA genotyping. The MHC-I class prediction algorithms included the NetMHC, NetMHCpan, PickPocket, SMM, and SMMPMBEC modules. HLA-corrected TMB was determined as previously reported.[8]

RNA extraction and sequencing data analysis

RNA was extracted using an RNeasy FFPE Kit (Qiagen), and ribosomal RNAs were removed using an NEBNext

rRNA Depletion Kit (New England Biolabs). The NEBNext Ultra II Directional RNA Library Prep Kit for Illumina (New England Biolabs) was used for library preparation. RNA sequencing was conducted on a NovaSeq 6000 system (Illumina). Adaptor sequences, low-quality reads, and reads with a high N ratio were removed using fastp (V.0.20.0). The remaining clean reads were aligned to ribosomal RNA sequences to remove ribosomal reads using bowtie2-2.2.8 and were further aligned to the human reference genome (GRCh37) using STAR software with default parameters.

Differentially expressed genes and gene set enrichment analysis

We used the R DESeq2 package to calculate the fold-changes between the PMME and NEMM subtypes. The false discovery rate (FDR) method was used to adjust the p values for multiple testing. Genes with an adjusted p value of less than 0.01 and |log2(fold-change)| > 2 were considered as significantly differentially expressed. Enrichment analysis was performed using the R clusterprofiler package, and pathways with an adjusted p value less than 0.05 and absolute value of normalized enrichment score greater than 1 were considered as significant.

mIHC staining

mIHC staining was conducted using a PANO 7-plex IHC kit (Panovue, Beijing, China). The slides were blocked and then incubated sequentially with CD8 (C8/144B, Cell Signaling Technology, Danvers, Massachusetts, USA), PD-L1 (E1L3N, Cell Signaling Technology), and SOX10 (EPR4007, Abcam, Cambridge, UK). The nuclei were counterstained with 4′,6-diamidino-2-phenylindole (Sigma-Aldrich, St. Louis, Missouri, USA). Multispectral images were obtained using a Mantra System (Perkin-Elmer, Waltham, Massachusetts, USA), and digital images were analyzed using inForm image analysis software (PerkinElmer).

Statistical analysis

Categorical variables were summarized as frequencies and percentages and analyzed using Pearson's χ^2 test or Fisher's exact test. Continuous variables were summarized as the median and range and compared between groups using the two-tailed unpaired Student's t-test or Wilcoxon test. Kaplan-Meier analysis was used to estimate the PFS and OS, which were compared using the log-rank test. Multivariate logistic regression analysis was used to adjust for potential confounders and estimate ORs and the 95% CI. Multivariable Cox proportional hazards regression models were used to adjust for potential confounders and estimate HRs and the 95% CI. All statistical analyses were two sided, and the significance level was set at 0.05. Statistical analyses were performed using R V.3.6.3 (The R Project for Statistical Computing, Vienna, Austria), SPSS software V.26.0 (SPSS), and GraphPad Prism V.8 software (GraphPad, La Jolla, California, USA).

Table 1 Patient demographics and baseline characteristics of patients administered anti-PD-1 (n=92)

Characteristics	PMME (n=28)	NEMM (n=64)
Sex		
Female	11 (39.3)	48 (75.0)
Male	17 (60.7)	16 (25.0)
Age, years	60 (42–74)	57 (27–79)
≤55	9 (32.1)	30 (46.9)
>55	19 (67.9)	34 (53.1)
Metastases		
M0	3 (10.7)	18 (28.1)
M1	25 (89.3)	46 (71.9)
Previous systemic therapy		
No	11 (39.3)	22 (34.4)
Yes	17 (60.7)	42 (65.6)
LDH		
Normal	20 (71.4)	48 (75.0)
Elevated	8 (28.6)	16 (25.0)
ECOG		
0	12 (42.9)	34 (53.1)
1	16 (57.1)	30 (46.9)

ECOG, Eastern Cooperative Oncology Group; LDH, lactate dehydrogenase; NEMM, non-esophageal mucosal melanomas; PMME, primary malignant melanoma of the esophagus.

RESULTS

PMME exhibited a better response to anti-PD-1 monotherapy compared with NEMM

In total, 92 patients with advanced mucosal melanoma were treated with anti-PD-1 monotherapy, including 28 patients with PMME and 64 with NEMM (26 genital, 25 nasal/oral, 12 anorectal, and 1 conjunctival). The basic patient characteristics are listed in table 1. The ORR of PMME (9/27, 33.3% (95% CI 14.3% to 52.3%)) was significantly higher than that of NEMM (4/61, 6.6% (95% CI 0.2% to 12.9%); p=0.002); similar results were observed for the DCR (20/27, 74.1% (95% CI 56.4% to 91.7%) in PMME, vs 23/61, 37.7% (95% CI 25.2% to 50.2%) in NEMM; p=0.002). PMME remained independently correlated with a better ORR (OR, 6.660 (95% CI 1.568 to 28.284); p=0.010) and DCR (OR, 8.478 (95% CI 2.421 to 29.691); p=0.001) in the multivariate logistic regression model (table 2). The median follow-up times of PMME and NEMM were 34.4 weeks (range, 10.6–222.0 weeks) and 43.0 weeks (range, 5.9–309.0 weeks), respectively. Although PMME and NEMM showed no significant difference in both PFS and OS (table 2, online supplemental figure 1A,B), the median PFS of PMME (32.0, 95% CI 17.8 to 46.2 weeks) was longer than that of NEMM (13.0, 95% CI 7.8 to 18.2 weeks).

Table 2 Best response and survival outcomes to anti-PD-1 treatment

Variables		PMME (n=28)	NEMM (n=64)
Response, No. (%)			
CR		0 (0)	1 (1.6)
PR		9 (32.1)	3 (4.7)
SD		11 (39.3)	19 (29.7)
PD		7 (25.0)	38 (59.4)
NE*		1 (3.6)	3 (4.7)
ORR†			
No. (%)		9 (33.3)	4 (6.6)
95% CI, %		14.3 to 52.3	0.2 to 12.9
Univariate *P* value		0.002	
Multivariate‡	P value	0.010	
	OR (95% CI)	6.660 (1.568 to 28.284)	
DCR§			
No. (%)		20 (74.1)	23 (37.7)
95% CI, %		56.4 to 91.7	25.2 to 50.2
Univariate p value		0.002	
Multivariate‡	P value	0.001	
	OR (95% CI)	8.478 (2.421 to 29.691)	
PFS			
Median (95% CI), weeks		32.0 (17.8 to 46.2)	13.0 (7.8 to 18.2)
Univariate	P value	0.311	
	HR (95% CI)	0.787 (0.495 to 1.251)	
Multivariate¶	P value	0.234	
	HR (95% CI)	0.589 (0.246 to 1.409)	
OS			
Median (95% CI), weeks		40.0 (27.1 to 52.9)	42.0 (23.3 to 60.7)
Univariate	P value	0.512	
	HR (95% CI)	1.178 (0.708 to 1.960)	
Multivariate¶	P value	0.584	
	HR (95% CI)	0.781 (0.323 to 1.892)	

*Patients not evaluable for response: two patients died before the evaluation of the disease and two patients were lost to follow-up.
†ORR = (CR + PR)/(CR + PR + SD + PD) × 100%.
‡Multivariate logistic regression analysis adjusted for age (>55 vs ≤55), sex (male vs female), baseline LDH level (elevated vs normal), baseline ECOG (1 vs 0), distant metastasis (with vs without), and prior systemic treatment (yes vs no).
§DCR = (CR + PR + SD)/(CR + PR + SD + PD) × 100%.
¶Other covariates included in the multivariate Cox proportional hazard regression model of PFS and OS were age, sex, baseline LDH level, baseline ECOG, distant metastasis, and previous systemic treatment.
CR, complete response; DCR, disease control rate; ECOG, Eastern Cooperative Oncology Group; LDH, lactate dehydrogenase; NE, not evaluable; NEMM, non-esophageal mucosal melanomas; ORR, overall response rate; OS, overall survival; PD, progressive disease; PFS, progression-free survival; PMME, primary malignant melanoma of the esophagus; PR, partial response; SD, stable disease.

Molecular and cellular underpinning strategy

To determine the genomic characteristics and gain insights into the mechanism of the outstanding response of PMME to anti-PD-1 compared with that of NEMM, we collected fresh frozen or FFPE samples of primary tumors from 23 patients with PMME and 45 patients with NEMM. The genomic and transcriptomic signatures were explored via next-generation sequencing; we also assessed the expression level of PD-L1 and infiltration of $CD8^+$ T cells using mIHC. The basic patient characteristics and results of specific molecular underpinning analysis are listed in online supplemental table 1, and the sample number of each analysis is shown in online supplemental figure 2.

PMME and NEMM display different mutational signatures

Genomic sequencing was performed in 21 patients with PMME and 23 with NEMM (figure 1A), and the detailed sequencing information is listed in online supplemental table 2. The median TMB of PMME and NEMM was numerically similar (both 2.0 mutations/Mb, range 0.5–11.7 and 0.6–7.8, respectively; p=0.805; online supplemental figure 3A). Similarly, no significant difference was

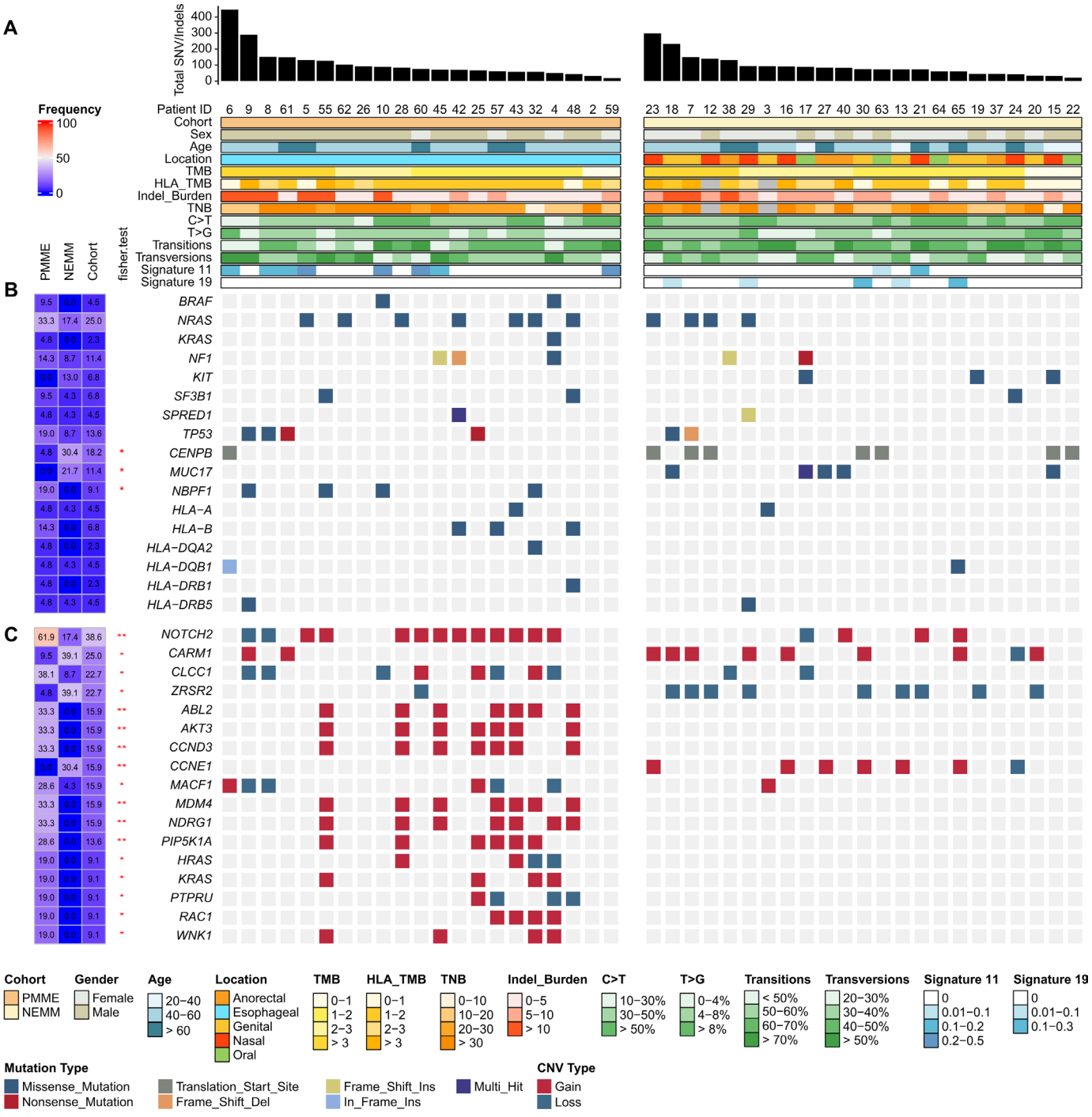

Figure 1 Overview of clinical and genetic characteristics of primary malignant melanoma of the esophagus (PMME) and non-esophageal mucosal melanoma (NEMM). (A) Overview of PMME (n=21) and NEMM samples (n=23) showing total number of single-nucleotide variations (SNVs) and insertions/deletions (indels), tumor mutational burden (TMB) using mutations (SNVs and indels) per megabase, human leukocyte antigen-corrected tumor mutation burden (HLA-TMB), indel burden, tumor neoantigen burden (TNB), and proportions of significantly different mutational processes. The patient ID, sex, age, and locations of the primary lesions in each sample are shown beneath the bar plot. (B) Oncoplot of mutations in classical melanoma driver genes, significantly mutated genes, and HLA class I and class II genes. (C) Oncoplot of copy number variations (CNVs) in significantly different genes. *Genes significantly different between PMME and NEMM (Fisher's exact test, *p<0.05, **p<0.01).

observed between PMME and NEMM in terms of indel burden (p=0.706), HLA-corrected TMB (p=0.734), and TNB (p=0.314; online supplemental figure 3B–D).

As shown in online supplemental figure 3E–H and online supplemental figure 4, PMME harbored more transversions (Tv, p=0.015) and fewer transitions (Ti, p=0.015) than NEMM; specifically, PMME exhibited a significantly lower fraction of C>T Ti (p=0.013) and T>G Tv (p=0.042) and higher fraction of C>G Tv (p=0.091). In PMME, the most prevalent signatures were

age-related signature 1, homologous recombination deficiency-related signature 3, immunoglobulin gene hypermutation-related signature 9 (all 9/21, 42.9%), and alkylating agents-related signature 11 (8/21, 38.1%). In NEMM, the most prevalent signatures were signature 1 (18/23, 78.3%), signature 3 (12/23, 52.2%), liver cancer-related signature 12 (11/23, 47.8%), and signature 16 (11/23, 47.8%). Signature 1 is reported to be negatively associated with immune activity and prognosis following immune checkpoint inhibitor therapy in melanoma.[14] Although signature 1 is the most common signature in both PMME and NEMM, its frequency was significantly lower in PMME than in NEMM (p=0.029). Furthermore, the TMB was lower in patients with PMME with signature 1 (median 1.53, range 0.47–2.71) than in those without it (median 2.88, range 1.32–11.74; p=0.009); however, no differences were found in the NEMM cohort (median 1.75, range 0.55–7.84 vs median 1.92, range 0.89–2.47; p=0.787; online supplemental figure 3I). The contribution of each signature was further analyzed, and the results showed that the contribution of signature 11 was significantly higher in PMME (p=0.014), whereas that of signature 19 was significantly higher in NEMM (p=0.025; online supplemental figure 3J–L).

PMME contains more aberrations in canonical driver genes than NEMM

Melanoma is typically classified into four mutational subtypes: *BRAF*-mutated, *RAS*-mutated, *NF1*-mutated, and triple wild-type.[15] In our study, approximately half of the PMME cases harbored mutations in *BRAF*, *N/KRAS*, and *NF1* (10/21, 47.6%), whereas most NEMM cases were triple wild-type (17/23, 73.9%; figure 1B). *N/KRAS* was the most frequently mutated gene in PMME (8/21, 38.1%), compared with a mutation rate of 17.4% (4/23) in NEMM. *TP53* was the second most frequently mutated driver gene in PMME with a mutation frequency of 19.0% (4/21) compared with 8.7% (2/23) in NEMM. *KIT* was mutated in 13.0% (3/23) of NEMM, whereas no *KIT* mutation was found in the PMME cohort. *SF3B1*, which was thought to be commonly mutated in anorectal and genital melanomas but rare in mucosal melanomas from other sites, was mutated in 9.5% (2/21) of PMME cases. Three genes were significantly differently mutated between the two cohorts. The centromere-coding gene *CENPB* and a mucin-coding gene *MUC17* were more prone to be mutated in NEMM, whereas a neuroblastoma breakpoint family member *NBPF1* mutation was only found mutated in PMME (4/21, 19.0%). The somatic mutation profiles are listed in online supplemental table 3.

Seventeen significantly different CNVs were identified between the two cohorts (figure 1C). Most PMME-enriched CNVs were copy number gain in receptor-coding or kinase-coding genes which can activate downstream signaling and promote cell proliferation, including a Notch pathway receptor (*NOTCH2*), GTPases (*HRAS*, *KRAS*, and *RAC1*), a lipid kinase (*PIP5K1A*), tyrosine or serine/threonine kinases (*ABL2*, *AKT3*, and *WNK1*), and a p53 inhibitor (*MDM4*). The different mutational landscape between the two cohorts indicated that the driving molecular events in PMME differ from those in NEMM, and PMME harbored more aberrations in canonical driver genes than NEMM.

PMME contains less loss-of-function aberrations in *JAK1/2* but more mutations in neurodevelopment or neurodegenerative-related genes than NEMM

Analysis of the genomic difference between PMME and NEMM in immune-related genes showed that 19.0% (4/21) of PMME cases harbored the *HLA-I* mutation, whereas only 4.3% (1/23) of NEMM cases harbored this mutation (figure 1A). Heterozygosity at the *HLA-I* loci (*HLA-A*, *HLA-B*, and *HLA-C*) was further analyzed; the results showed that 26.1% (6/23) of NEMM cases were homozygous in at least one *HLA-I* locus, which was higher than the rate observed in PMME (2/21, 9.5%). Gene alterations in signaling pathways previously reported to be associated with ICB sensitivity[8–10 16 17] were further compared between PMME and NEMM (figure 2A). Loss-of-function mutation or copy number loss in *JAK1/2* was found in 28.6% (6/21) of PMME cases and 47.8% (11/23) of NEMM cases. In the 10 PMME cases subjected to genome and transcriptome sequencing, we performed gene set enrichment analysis (GSEA); the results showed that JAK/STAT signaling and immune-related genes were more enriched in cases with normal *JAK1/2* (figure 2B). The PMME cohort contained more variations in the PTPR family, which can dephosphorylate and inactivate JAKs, indicating that the signaling activity of JAK/STAT is higher in PMME than in NEMM. For β-catenin signaling, NEMM tends to show higher copy number gain in genes regulating β-catenin degradation (*APC2*, *AXIN1*, and *AXIN2*). No significant difference was observed in the DNA repair, CDK4 pathway or *PTEN*.

By comparing the top 20 mutated genes in each cohort (online supplemental figure 5), we found that PMME harbored more mutations in neurodevelopmental or neurodegenerative disease-related genes (*NBPF1*, *DPF1*, *MACF1*, *MAOB*, *MYCBP2*, and *RNF40*). We investigated the impact of mutations in these genes on the efficacy and survival of patients treated with anti-PD-1 in three published clinical cohorts,[18–20] and found that the response rate was significantly higher in patients harboring these mutations than in patients without mutations (52.8% (95% CI 38.9% to 66.7%) vs 33.5% (95% CI 26.6% to 40.4%), p=0.015; online supplemental figure 6A), particularly *NBPF1* (75.0% (95% CI 46.3% to 103.7%) vs 35.8% (95% CI 29.5% to 42.1%), p=0.011; online supplemental figure 6B). In addition, the six genes mutant patients tended to have a longer PFS (mPFS 9.3, 95% CI 0 to 31.5 months vs 3.6, 95% CI 1.2 to 6.0 months; HR 0.73, 95% CI 0.46 to 1.17; p=0.226) and a significantly longer OS (mOS not reached vs 24.7, 95% CI 19.0 to 30.4 months; HR 0.52, 95% CI 0.34 to 0.79; p=0.011), particularly *NBPF1* and *MYCBP2* (online supplemental figure

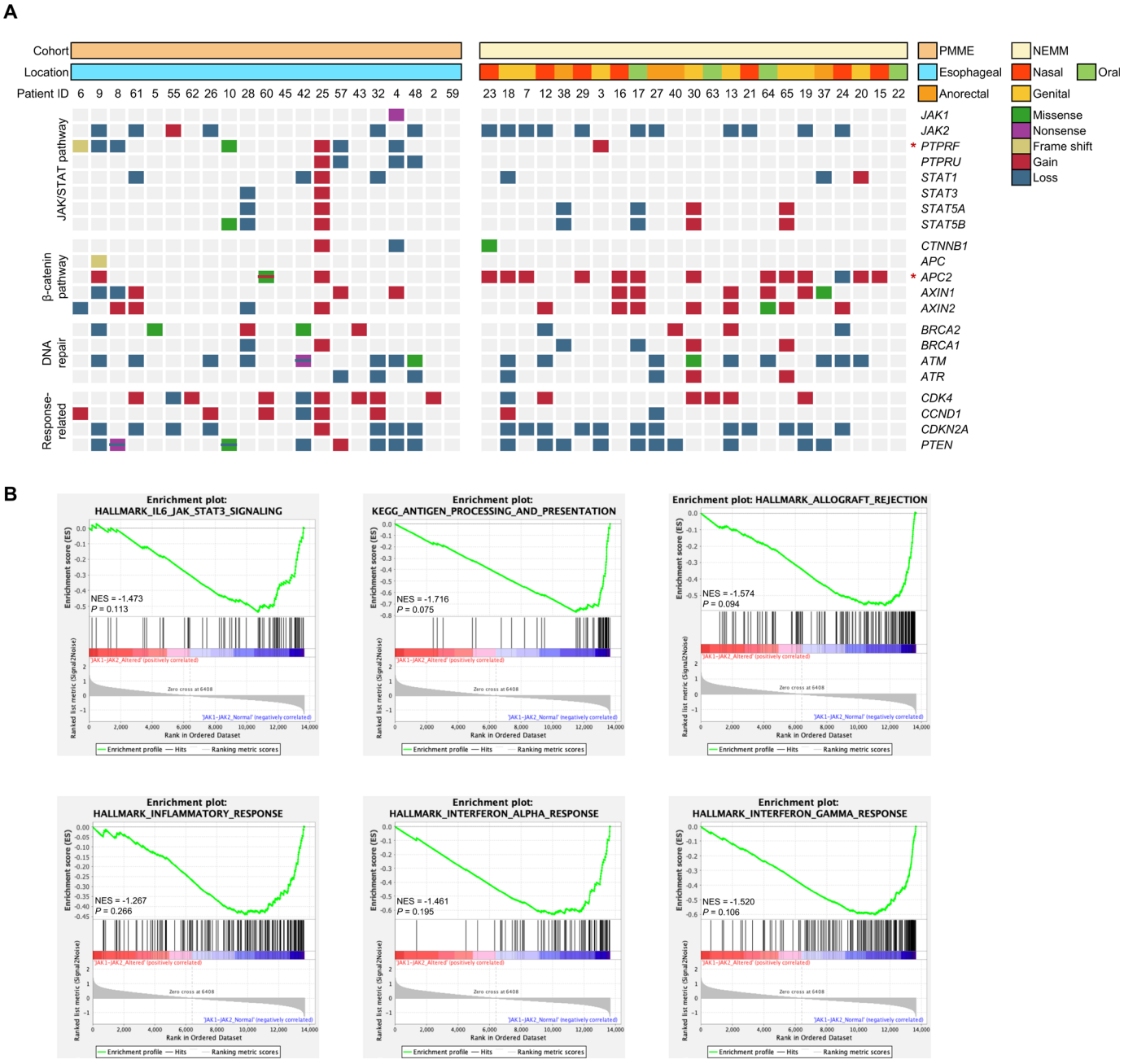

Figure 2 Somatic alterations in reported immune checkpoint sensitivity related genes. (A) Oncoplot of somatic alterations (including mutations and copy number variations) in reported response genes with at least one somatic aberration. (B) Gene set enrichment analysis (GSEA) plot of the gene sets in IL6-JAK-STAT3, antigen processing and presentation, allograft rejection, inflammatory response, interferon alpha, and interferon gamma, identified as significantly enriched (adjusted p<0.05) using unbiased GSEA. *Genes significantly different between PMME and NEMM (Fisher's exact test, *p<0.05).

6C–H). These results indicated that mutations in neurodevelopmental or neurodegenerative disease-related genes may be a predictor of good response to anti-PD-1 therapy.

PMME exhibits a less immunosuppressive but more proliferation signature than NEMM

RNA sequencing was performed in 10 PMME and 24 NEMM fresh frozen samples to further evaluate transcriptome signature differences between PMME and NEMM. CIBERSORT was used to estimate the immune cell infiltration differences between the two cohorts (figure 3A). We observed a higher proportion of $CD8^+$ T cells (Mann-Whitney U test unadjusted p=0.009, FDR-adjusted p=0.060) and activated DCs (Mann-Whitney U test unadjusted p=0.006, FDR-adjusted p=0.062) in PMME. We then explored the expression of genes related to T-cell activity or response to ICB and found that PMME showed higher expression of several markers of T-cell cytotoxicity and HLA-I antigen presentation than NEMM (figure 3A). Although the expression of PD-L1 and PD-L2

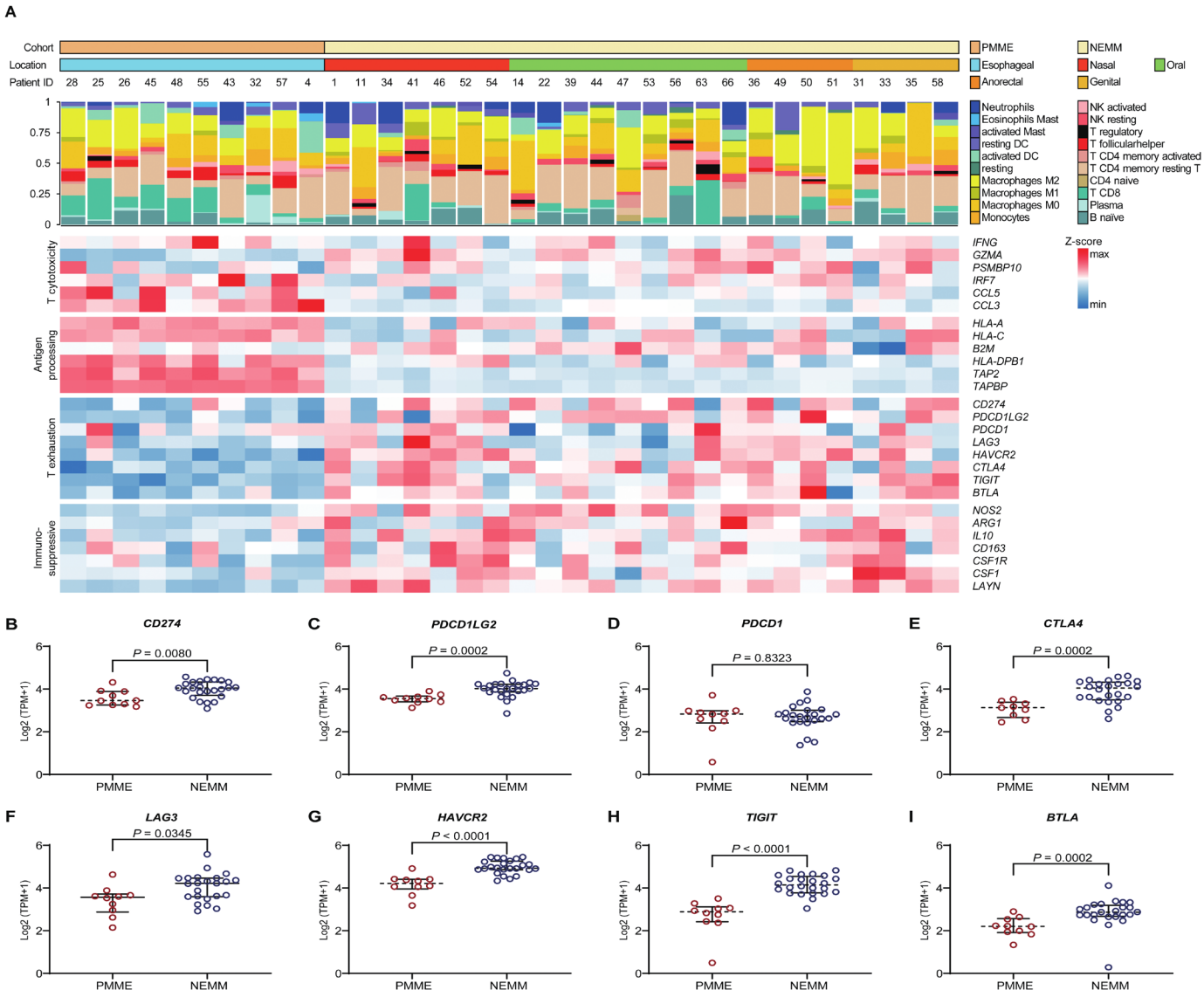

Figure 3 Primary malignant melanoma of the esophagus (PMME) displays a more inflammatory tumor microenvironment than non-esophageal mucosal melanoma (NEMM). (A) Immune cell infiltration differences between PMME and NEMM were measured using the CIBERSORT method. Expression of several markers of T-cell cytotoxicity and exhaustion, human leukocyte antigen (HLA)-I antigen presentation, and immunosuppressive markers in myeloid cells are shown. Each column represents individual patients. (B–G) Expression differences of immune checkpoints in PMME and NEMM.

were reported to be positively associated with the response to anti-PD-1, the expression of *CD274* (encoding PD-L1) and *PDCD1LG* (encoding PD-L2) were significantly lower in PMME than in NEMM (figure 3B,C). Except for *PDCD1* (p=0.8323, figure 3D), which encodes the receptor for PD-L1 and PD-L2, the expression levels of most other inhibitory immune checkpoints expressed on T cells, such as *CTLA4*, *LAG3*, *HAVCR2* (encoding TIM3), *TIGIT*, *BTLA*, were lower in PMME than in NEMM (figure 3E–I). PMME also showed lower expression of immunosuppressive markers in myeloid cells than NEMM, indicating a less immunosuppressive molecular signature.

GSEA was performed to identify other biological differences between the two cohorts to provide insight into why PMME is more aggressive than NEMM but showed a better clinical benefit from anti-PD-1 monotherapy. DNA repair-related and telomerase-related gene sets were significantly enriched in PMME, whereas myeloid cell-mediated immunity-related and metabolic process-related gene sets were more enriched in NEMM (figure 4A,B). We found that the expression levels of the melanoma proliferative phenotype-associated genes, *MITF*, *PAX3*, *FOXD3*, *ETV1*, *TBX2*, *SOX9*, *TRPM1*, *PARP1*, and *ZEB2*, were significantly higher in PMME than in NEMM (figure 4C). Cell cycle pathway checkpoint *CDK4* was upregulated and its inhibitors *CDKN1A* and *CDKN2A* were downregulated in PMME. *MITF* and its upstream *PAX3* and *FOXD3* regulate the proliferation of melanocytes and melanoma but are also the main modulators of melanocyte differentiation.[21] Dedifferentiation and loss of melanocyte differentiation antigens can result in resistance to immunotherapy[22]; therefore, the melanocyte differentiation-related genes

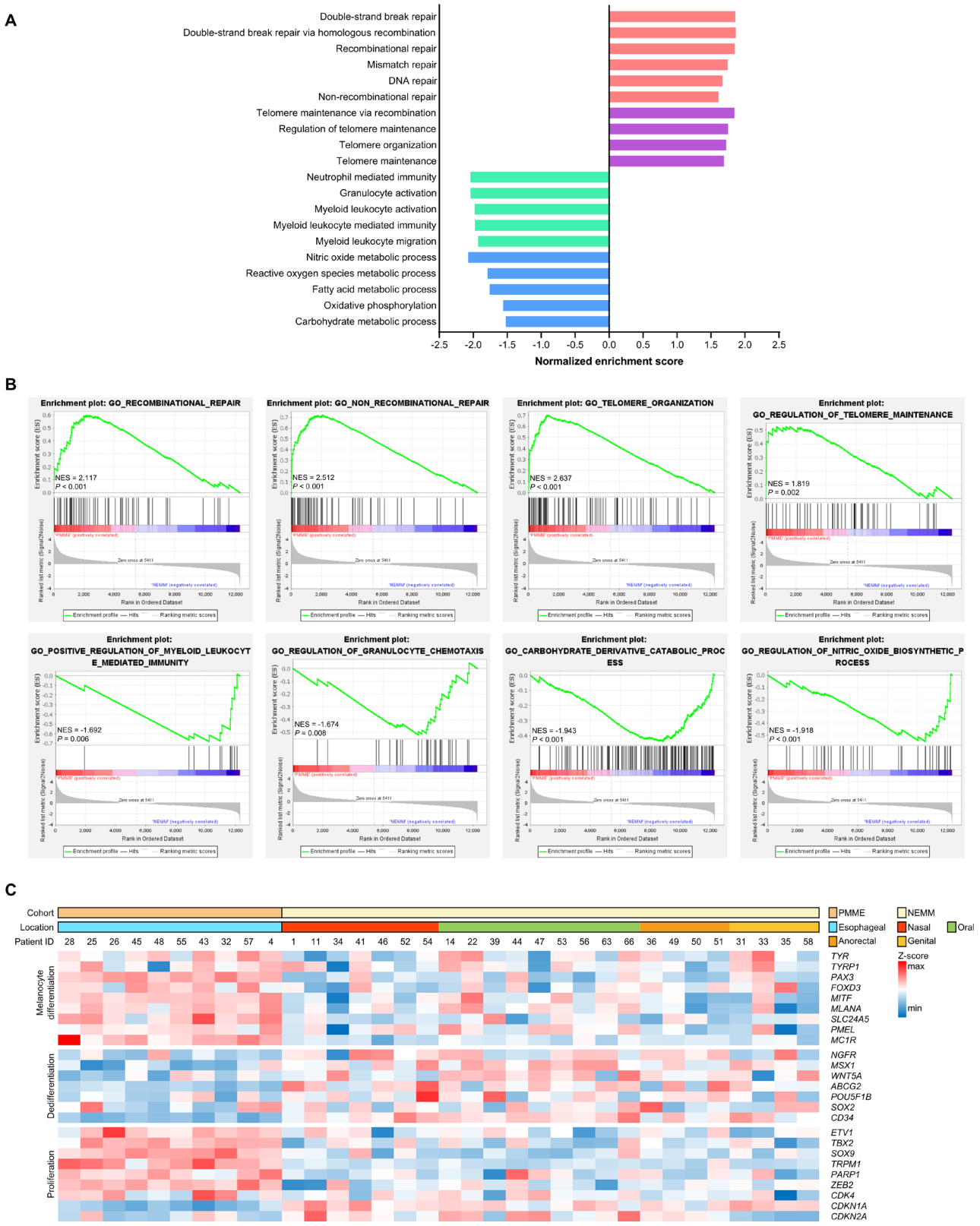

Figure 4 Primary malignant melanoma of the esophagus (PMME) shows a higher proliferative and differentiated character than non-esophageal mucosal melanoma (NEMM). (A, B) Gene set enrichment analysis (GSEA) was performed to detect biological differences between the two cohorts. (A) DNA repair-related and telomerase-related gene sets were significantly enriched in PMME, and myeloid cell-mediated immunity-related and metabolic process-related gene sets were more enriched in NEMM. Pathways with an adjusted p value less than 0.05 and absolute value of normalized enrichment score greater than one were considered as significant. (B) Selected GSEA plots of gene sets in DNA repair, telomerase, myeloid cell-mediated immunity, and metabolic process. (C) Heatmap of melanocyte differentiation, dedifferentiation, and proliferation genes with a significant difference between PMME and NEMM.

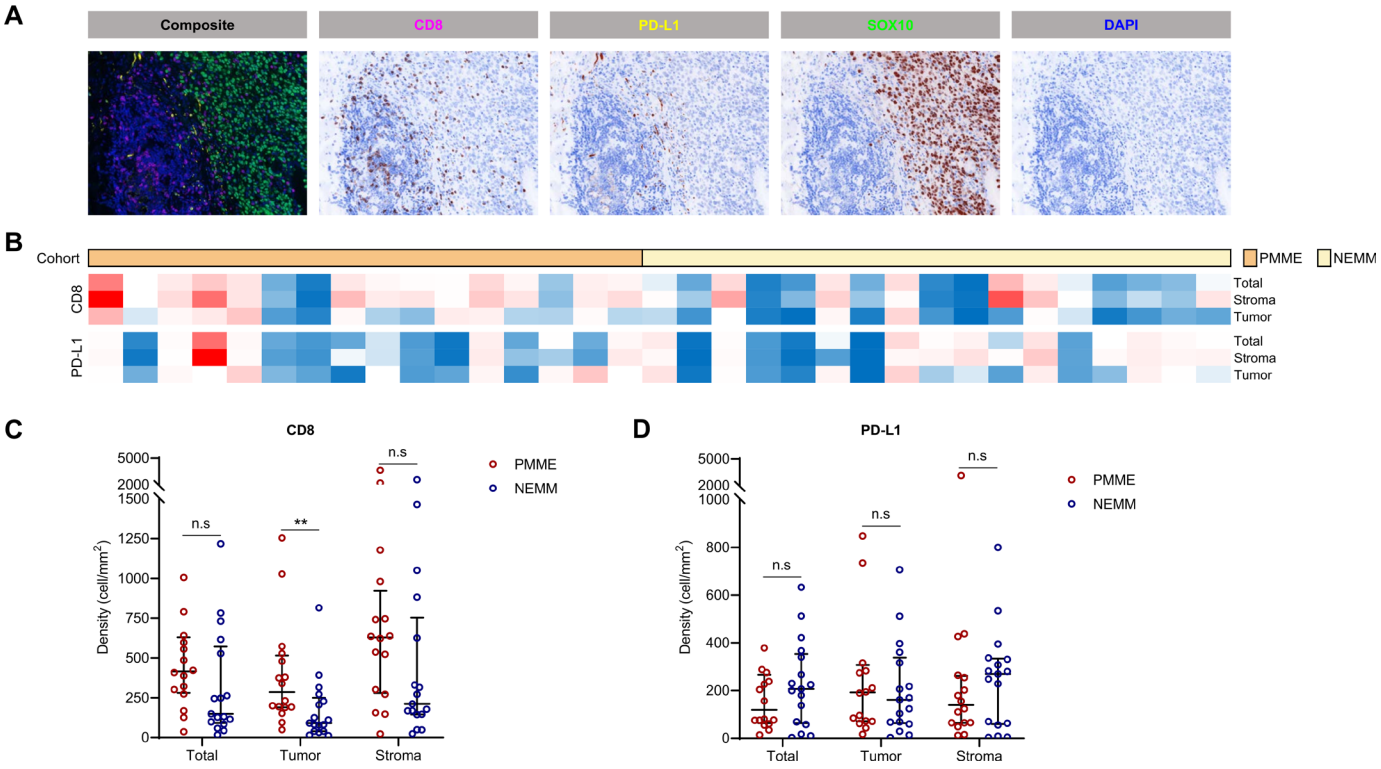

Figure 5 Primary malignant melanoma of the esophagus (PMME) has more infiltrating CD8$^+$ T cells than non-esophageal mucosal melanoma (NEMM). (A) Representative multiplex immunohistochemistry (IHC) of CD8 and PD-L1 expression. (B) Heatmap of CD8 and PD-L1 expression in the tumor, stroma, and whole slides. Each column represents individual patients grouped according to cohorts. (C) Density (cells/mm^2) differences in CD8 and PD-L1 expression in the tumor, stroma, and whole slides (Wilcoxon, *p<0.05, **p<0.01).

were further compared. PMME expressed higher levels of melanocyte differentiation genes (*TYR*, *TYRP1*, *PAX3*, *FOXD3*, *MITF*, *MLANA*, *SLC24A5*, *PMEL*, and *MC1R*), and NEMM showed a more dedifferentiation feature with higher expression of neural crest cell and stem cell markers (*NGFR*, *MSX1*, *WNT5A*, *ABCG2*, *POU5F1B*, *SOX2*, and *CD34*) than NEMM.

More CD8$^+$ T cells infiltrate in PMME than in NEMM

The infiltration of CD8$^+$ T cells as well as PD-L1 expression in 16 PMME and 17 NEMM samples were further examined using mIHC staining, and SOX10 was used to label melanoma cells (figure 5A). The intratumoral densities of CD8$^+$ T cells were significantly higher in PMME than in NEMM, and the densities of CD8$^+$ T cells in the stromal area and total slides tended to be higher in PMME than in NEMM (figure 5B,C), which was in accordance with the CIBERSORT estimation based on transcriptome sequencing. These results indicate that PMME had higher CD8$^+$ T-cell infiltration in the tumor microenvironment than NEMM. Inconsistent with the lower *CD274* level in PMME, the expression level of PD-L1 did not significantly differ between PMME and NEMM (figure 5B,D).

DISCUSSION

Most reported ORRs to anti-PD-1 monotherapy in mucosal melanoma were below 25%, which is considerably lower than those for cutaneous melanoma.[23–25] Compared with patients with cutaneous melanoma, patients with mucosal melanoma have a shorter PFS of 1.4–10.2 months and median OS of 8.2–20.1 months following anti-PD-1 treatment.[26] However, patients with PMME have not been widely examined, possibly because of the extremely low incidence of this subtype. We retrospectively analyzed patients with PMME and NEMM treated with anti-PD-1 monotherapy. The results revealed an ORR and DCR of 33.3% and 74.1%, respectively, for patients with PMME, which was significantly higher than the values in our NEMM cohort. Sheng *et al* reported that the anti-PD-1 antibody toripalimab combined with the vascular endothelial growth factor receptor inhibitor axitinib could improve the ORR up to 48.3% in mucosal melanoma. In this clinical trial, a better clinical response was also observed in PMME.[27]

Although PMME showed a better response and longer median PFS than NEMM, the OS after anti-PD-1 monotherapy was comparable between PMME and NEMM, which may be the result of PMME being more aggressive.[2–4] In our cohort, the DFS of patients with PMME (median 25.7 (95% CI 19.5 to 31.9) weeks) was significantly shorter than that of patients with NEMM (median 37.6 (95% CI 24.5 to 50.7) weeks) in multivariate Cox regression analysis after adjusting for age, sex, LDH at diagnosis, local metastasis, ECOG at diagnosis, and

adjuvant treatment (HR 2.654 (95% CI 1.085 to 6.489); p=0.032), establishing that PMME was more malicious than NEMM. Therefore, we speculated that the superior response rate of PMME did not produce a survival benefit over NEMM because PMME is more aggressive and progresses faster than NEMM. From another perspective, the poorer survival of PMME was reversed as anti-PD-1 monotherapy prolonged the OS of PMME to a similar level as that of NEMM.

Through assembled multiomics profiling, we analyzed the molecular differences between PMME and NEMM to explore their mechanisms. At the genomic level, a higher TMB, indel burden, TNB, and HLA-corrected TMB were reported to be correlated with a better response to ICB.[6–8] In our study, the mutation burden was low in both PMME and NEMM, with no difference observed in these terms. The mutational signatures are the footprints of endogenous and exogenous mutagenic factors that may reveal the etiology of cancer. In our study, the most prominent signatures in PMME were signatures 1, 3, 9, and 11; those in NEMM were signatures 1, 3, 12, and 16, supporting that signature 1 was the most important signature in mucosal melanoma.[28] Furthermore, the TMB was significantly higher in PMME cases with signature 1 than in those without this signature, which corresponds with the findings of Chong *et al* in cutaneous melanoma.[14] However, the TMB did not differ in patients with NEMM with or without signature 1. Signature 11 is most commonly found in melanoma and glioblastoma and is associated with mismatch repair deficiency and a higher TMB.[29] The three most active signatures in cutaneous melanoma were signatures 1, 7, and 11.[30] PMME contained more mutations in classical cutaneous melanoma driver genes, and only 52.4% of PMME cases was triple wild-type. The mutational signature and driver genes reflect those reported by Li *et al*, who found that PMME had similar genomic patterns as cutaneous melanoma.[31] Overall, similar genomic patterns with cutaneous melanoma may explain why PMME exhibited a more favorable response to anti-PD-1 treatment than NEMM.

NRAS was the most frequently mutated gene in PMME, with a mutation rate of 33.3%, which was higher than that in NEMM and is consistent with previous reports showing that *NRAS* is the most commonly mutated gene in PMME.[32 33] *N/KRAS* and *TP53* were reported to be correlated with a better response to ICB in melanoma and lung cancer.[34–36] In our study, 57.1% (12/21) of PMME cases harbored an *N/KRAS* or *TP53* mutation, which was significantly higher than that in NEMM (5/23, 21.7%, p=0.029). One reason that patients with *NRAS* mutations were more likely to benefit from ICB is that *NRAS* mutant melanoma is associated with a higher mutational burden and *NRAS*-mutated melanoma showed a higher proportion of PD-L1-positive cells.[35] *KRAS* is correlated with an inflammatory phenotype and favorable clinical benefit of anti-PD-1/PD-L1 immunotherapy for non-small cell lung cancer.[36] *N/K/HRAS* are the most important drivers of tumorigenesis and are activated by mutation in 15% of human cancers, and melanoma harboring *NRAS* is more aggressive than $BRAF^{V600E}$-mutated and wild-type melanoma.[37] The higher response rate of *NRAS*-mutated melanoma did not translate into a survival benefit. We previously retrospectively analyzed the association of *NRAS* mutation status with the clinical outcomes of anti-PD-1 monotherapy in advanced melanoma, which showed that the PFS and OS of patients with *NRAS* mutation were shorter than those of patients without *NRAS* mutation in cutaneous and acral/mucosal melanoma.[38] Kirchberger *et al* also reported that survival is less favorable in immune checkpoint inhibitor-treated patients with *NRAS* mutation.[39] Therefore, the high mutation frequency of *RAS* family might be another reason for a better response to anti-PD-1 and the highly aggressive nature of PMME compared with NEMM.

Loss-of-function mutation in *JAK1/2* may induce acquired resistance to ICB in melanoma, possibly because *JAK1/2* mutations caused melanoma cells to lose the ability to respond to interferon γ and prevented PD-L1 expression.[9] In our study, compared with NEMM, PMME harbored lower levels of loss-of-function mutation or copy number loss in *JAK1/2*, and PMME with a normal *JAK1/2* genotype displayed higher JAK/STAT signaling enrichment and more inflammatory transcriptome signatures, indicating that a lower *JAK1/2* aberration frequency leads to a stronger response to anti-PD-1 in PMME. In addition to a larger number of *RAS* mutations and smaller number of *JAK1/2* alterations, PMME showed higher *HLA-I* heterozygosity and higher expression of antigen-presenting machinery-related genes than NEMM. Transcriptional downregulation of *HLA-I* molecules on melanoma cells was associated with resistance to ICB, and *MHC-I*-low tumors displayed reduced T-cell infiltration and a myeloid cell-enriched microenvironment.[40 41] Therefore, enhanced antigen procession and presentation may be the fourth reason for the exceptional response to anti-PD-1 of PMME. Furthermore, a higher proportion of $CD8^+$ T cells, lower expression of T exhaustion markers, and less immunosuppressive and myeloid cell signature were observed in PMME, indicating that a more inflammatory microenvironment is the fifth reason for these results.

Activation of Wnt/β-catenin signaling is reportedly to be associated with ICB sensitivity.[16] However, NEMM showed a higher copy number gain in genes regulating β-catenin degradation than PMME, which contrasts the notion of an attenuated response to ICB. Grasso *et al* analyzed transcriptome tumor biopsies from patients with melanoma at baseline or during ICB therapy and found that ICB responders exhibited a significantly decreased Wnt activation score in on-therapy biopsies, whereas no change was observed in non-responders.[42] Therefore, the decline in Wnt/β-catenin signaling after treatment may be more crucial than the baseline aberration status and expression level. Notably, Wnt/β-catenin signaling plays a key role in melanocyte differentiation,[43] and dedifferentiation and loss of melanocyte differentiation antigens

can result in resistance to immunotherapy.[22] *NBPF1* was a significantly differently mutated gene between PMME and NEMM. This gene is involved in brain development and neuroblastoma onset and exerts tumor-suppressive effects in different cancers.[44–46] In addition to *NBPF1*, we found that PMME cases harbored a larger number of mutations in genes involved in brain and neurological system development, and these mutations were associated with clinical outcome of anti-PD-1 therapy. Furthermore, at the transcriptome level, PMME expressed higher levels of melanocyte differentiation genes, and NEMM showed more dedifferentiation features with higher expression of neural crest cell and stem cell markers. Accordingly, mutations in differentiation-related genes and a more differentiated phenotype may be the sixth reason for the better therapeutic response in PMME than in NEMM.

In addition to the above-mentioned genes related to the responses to anti-PD-1 therapy (*RAS*, *TP53*), other canonical oncogenic driver genes were frequently altered in PMME, particularly those associated with the signaling activity and malignancy of cancer. Amplification in *NOTCH2*, *MDM4*, *PIP5K1A*, *RAC1*, and *WNK1* was considerably more frequent in PMME than in NEMM. Newell *et al* reported that *NOTCH2* amplification was more common in the tumors of European patients than in those of East Asian patients.[28] Zou *et al* performed genomic profiling of Chinese patients with melanoma, including 54 acral melanomas and 13 mucosal melanomas, and reported that *NOTCH2* amplification was enriched in acral melanomas but was not detected in mucosal melanomas.[47] These data demonstrate that *NOTCH2* amplification is relatively rare in Chinese NEMM cases. *MDM4*, *PIP5K1A*, and *RAC1* are all associated with the function of RAS family.[48–50]Additionally, transcriptome analysis revealed greater enrichment of DNA repair-related and telomere maintenance-related genes in PMME, and the expression levels of proliferation markers were higher in PMME than in NEMM. Therefore, the high frequency of aberration in genes regulating various cancer signaling pathways and high proliferation characteristics in PMME may explain the more aggressive behavior and shorter DFS of PMME than those of NEMM.

This study had some limitations. First, because mucosal melanoma is rare, the number of patients receiving anti-PD-1 monotherapy was small, and most patients were administered multiple lines of treatment. Moreover, individual heterogeneity and drug discrepancy influenced the drawing of a solid conclusion. Further multicenter prospective studies including more patients with mucosal melanoma receiving the same anti-PD-1 therapy as first-line treatment are required to verify the superior response to anti-PD-1 therapy in PMME. Another limitation is that the multi-omics analysis samples were not from anti-PD-1 clinical trials, and because of the low sample volume, quality, and conservation method limitations, not all samples could be evaluated in all experiments. Therefore, we could not confirm the specific molecular mechanism underlying the improved response of PMME to ICB. In addition, we performed bulk RNA sequencing to analyze the transcriptome signature and evaluate the immune microenvironment, as it was difficult to acquire fresh PMME samples for single-cell RNA sequencing or mass cytometry, and some samples had been stored in liquid nitrogen for several years. Baseline and on-treatment biopsies from a prospective cohort analyzed via single-cell RNA sequencing and mass cytometry will provide a more accurate transcriptome landscape and immune infiltration feature of PMME, thereby revealing the specific mechanism of the improved ICB response in PMME.

Our results suggest that PMME differs from NEMM as PMME responds better to anti-PD-1 treatment, possibly because of its distinct pattern of genomic alterations, larger number of infiltrating $CD8^+$ T cells, higher antigen presentation, greater differentiation character, and lower expression of co-inhibitory molecules and immunosuppressive features. However, PMME harbored more mutations and amplifications in canonical driver genes than NEMM, leading to more aggressive behavior. Combination therapies to impair melanoma cell proliferation may further improve the survival of patients with PMME.

Author affiliations
[1]Key Laboratory of Carcinogenesis and Translational Research (Ministry of Education/Beijing), Department of Melanoma and Sarcoma, Peking University Cancer Hospital and Institute, Beijing, China
[2]State Key Laboratory of Microbial Resources, Institute of Microbiology, Chinese Academy of Sciences, Beijing, China
[3]GenePlus- Shenzhen Clinical Laboratory, Shenzhen, China
[4]Department of Medical Oncology, Fujian Cancer Hospital & Fujian Medical University Cancer Hospital, Fuzhou, Fujian, China
[5]Key Laboratory of Carcinogenesis and Translational Research (Ministry of Education/Beijing), Department of Genitourinary Oncology, Peking University Cancer Hospital and Institute, Beijing, China
[6]Geneplus-Beijing, Beijing, China

Acknowledgements We would like to thank the patients for consenting tumor acquisition. We also thank Dr. Jianming Ying from the Chinese Academy of Medical Sciences and Peking Union Medical College for data discussion.

Contributors JD, XB, LS, and LM designed and wrote the manuscript; LS is responsible for the overall content as the guarantor; JD, XB, XG, LT, ZX, and XX performed tissue sequencing and data analysis; JG, LS, XW, ZQ, YC, and CL collected clinical information and followed up the patients; YC, YK, CC, XS, ZC, BL, SL, XY, BT, LZ, and XW collected the specimens. All authors reviewed and approved the final manuscript.

Funding This work was supported by Beijing Natural Science Foundation (7202024 and 7214217), National Natural Science Foundation of China (82073011, 82272676, 81972562, and 81972566), Beijing Medical Award Foundation (YXJL-2020-0889-0106), and Beijing Municipal Administration of Hospitals' Ascent Plan (DFL20220901).

Competing interests JG serves as consultant or is on the advisory boards for MSD, Roche, Pfizer, Bayer, Novartis, Simcere Pharmaceutical Group, Shanghai Junshi Biosciences, and Oriengene. LS has received speakers' honoraria from MSD, Roche, Novartis, Shanghai Junshi Biosciences, and Oriengene. XB has received a merit award supported by BMS. None of these relationships involve the work described in this manuscript. No potential conflicts of interest were disclosed by the other authors.

Patient consent for publication Not applicable.

Ethics approval This study involves human participants and was approved by Peking University Cancer Hospital institutional review board (2016KT59). Participants gave informed consent to participate in the study before taking part.

Provenance and peer review Not commissioned; externally peer reviewed.

Data availability statement Data are available on reasonable request. All data relevant to the study are included in the article or uploaded as online supplemental information.

Supplemental material This content has been supplied by the author(s). It has not been vetted by BMJ Publishing Group Limited (BMJ) and may not have been peer-reviewed. Any opinions or recommendations discussed are solely those of the author(s) and are not endorsed by BMJ. BMJ disclaims all liability and responsibility arising from any reliance placed on the content. Where the content includes any translated material, BMJ does not warrant the accuracy and reliability of the translations (including but not limited to local regulations, clinical guidelines, terminology, drug names and drug dosages), and is not responsible for any error and/or omissions arising from translation and adaptation or otherwise.

Open access This is an open access article distributed in accordance with the Creative Commons Attribution Non Commercial (CC BY-NC 4.0) license, which permits others to distribute, remix, adapt, build upon this work non-commercially, and license their derivative works on different terms, provided the original work is properly cited, appropriate credit is given, any changes made indicated, and the use is non-commercial. See http://creativecommons.org/licenses/by-nc/4.0/.

ORCID iDs
Jie Dai http://orcid.org/0000-0001-7586-7889
Xue Bai http://orcid.org/0000-0002-5203-4080
Chuanliang Cui http://orcid.org/0000-0001-6455-0843
Xinan Sheng http://orcid.org/0000-0001-9359-0975
Bin Lian http://orcid.org/0000-0003-0090-1290
Bixia Tang http://orcid.org/0000-0002-3458-461X
Li Zhou http://orcid.org/0000-0002-9331-0600

REFERENCES

1 Lian B, Cui CL, Zhou L, *et al*. The natural history and patterns of metastases from mucosal melanoma: an analysis of 706 prospectively-followed patients. *Ann Oncol* 2017;28:868–73.
2 Gao S, Li J, Feng X, *et al*. Characteristics and surgical outcomes for primary malignant melanoma of the esophagus. *Sci Rep* 2016;6:23804.
3 Dai L, Wang Z, Xue Z. Results of surgical treatment for primary malignant melanoma of the esophagus: a multicenter retrospective study. *J Thorac Cardiovasc Surg* 2020;S0022-5223:30571–7.
4 Cui C, Lian B, Zhou L, *et al*. Multifactorial analysis of prognostic factors and survival rates among 706 mucosal melanoma patients. *Ann Surg Oncol* 2018;25:2184–92.
5 Carlino MS, Larkin J, Long GV. Immune checkpoint inhibitors in melanoma. *Lancet* 2021;398:1002–14.
6 Van Allen EM, Miao D, Schilling B, *et al*. Genomic correlates of response to CTLA-4 blockade in metastatic melanoma. *Science* 2015;350:207–11.
7 Turajlic S, Litchfield K, Xu H, *et al*. Insertion-and-deletion-derived tumour-specific neoantigens and the immunogenic phenotype: a pan-cancer analysis. *Lancet Oncol* 2017;18:1009–21.
8 Shim JH, Kim HS, Cha H, *et al*. HLA-corrected tumor mutation burden and homologous recombination deficiency for the prediction of response to PD-(L)1 blockade in advanced non-small-cell lung cancer patients. *Ann Oncol* 2020;31:902–11.
9 Shin DS, Zaretsky JM, Escuin-Ordinas H, *et al*. Primary resistance to PD-1 blockade mediated by *JAK1/2* mutations. *Cancer Discov* 2017;7:188–201.
10 Peng W, Chen JQ, Liu C, *et al*. Loss of PTEN promotes resistance to T cell-mediated immunotherapy. *Cancer Discov* 2016;6:202–16.
11 Mignard C, Deschamps Huvier A, Gillibert A, *et al*. Efficacy of immunotherapy in patients with metastatic mucosal or uveal melanoma. *J Oncol* 2018;2018:1–9.
12 Hayward NK, Wilmott JS, Waddell N, *et al*. Whole-genome landscapes of major melanoma subtypes. *Nature* 2017;545:175–80.
13 Kaunitz GJ, Cottrell TR, Lilo M, *et al*. Melanoma subtypes demonstrate distinct PD-L1 expression profiles. *Lab Invest* 2017;97:1063–71.
14 Chong W, Wang Z, Shang L, *et al*. Association of clock-like mutational signature with immune checkpoint inhibitor outcome in patients with melanoma and NSCLC. *Mol Ther Nucleic Acids* 2021;23:89–100.
15 Akbani R, Akdemir KC, Aksoy BA, *et al*. Genomic classification of cutaneous melanoma. *Cell* 2015;161:1681–96.
16 Spranger S, Bao R, Gajewski TF. Melanoma-intrinsic β-catenin signalling prevents anti-tumour immunity. *Nature* 2015;523:231–5.
17 Yu J, Yan J, Guo Q, *et al*. Genetic aberrations in the CDK4 pathway are associated with innate resistance to PD-1 blockade in Chinese patients with non-cutaneous melanoma. *Clin Cancer Res* 2019;25:6511–23.
18 Liu D, Schilling B, Liu D, *et al*. Integrative molecular and clinical modeling of clinical outcomes to PD1 blockade in patients with metastatic melanoma. *Nat Med* 2019;25:1916–27.
19 Riaz N, Havel JJ, Makarov V, *et al*. Tumor and microenvironment evolution during immunotherapy with nivolumab. *Cell* 2017;171:934–49.
20 Hugo W, Zaretsky JM, Sun L, *et al*. Genomic and transcriptomic features of response to anti-PD-1 therapy in metastatic melanoma. *Cell* 2016;165:35–44.
21 Kubic JD, Lui JW, Little EC, *et al*. PAX3 and FOXD3 promote CXCR4 expression in melanoma. *J Biol Chem* 2015;290:21901–14.
22 Mehta A, Kim YJ, Robert L, *et al*. Immunotherapy resistance by inflammation-induced dedifferentiation. *Cancer Discov* 2018;8:935–43.
23 Ogata D, Haydu LE, Glitza IC, *et al*. The efficacy of anti-programmed cell death protein 1 therapy among patients with metastatic acral and metastatic mucosal melanoma. *Cancer Med* 2021;10:2293–9.
24 D'Angelo SP, Larkin J, Sosman JA, *et al*. Efficacy and safety of nivolumab alone or in combination with ipilimumab in patients with mucosal melanoma: a pooled analysis. *J Clin Oncol* 2017;35:226–35.
25 Nomura M, Oze I, Masuishi T, *et al*. Multicenter prospective phase II trial of nivolumab in patients with unresectable or metastatic mucosal melanoma. *Int J Clin Oncol* 2020;25:972–7.
26 Li J, Kan H, Zhao L, *et al*. Immune checkpoint inhibitors in advanced or metastatic mucosal melanoma: a systematic review. *Ther Adv Med Oncol* 2020;12:1758835920922028.
27 Sheng X, Yan X, Chi Z, *et al*. Axitinib in combination with toripalimab, a humanized immunoglobulin G4 monoclonal$_4$antibody against programmed cell death-1, in patients with metastatic mucosal melanoma: An open-label phase IB trial. *J Clin Oncol* 2019;37:2987–99.
28 Newell F, Kong Y, Wilmott JS, *et al*. Whole-genome landscape of mucosal melanoma reveals diverse drivers and therapeutic targets. *Nat Commun* 2019;10:3163.
29 Touat M, Li YY, Boynton AN, *et al*. Mechanisms and therapeutic implications of hypermutation in gliomas. *Nature* 2020;580:517–23.
30 Conway JR, Dietlein F, Taylor-Weiner A, *et al*. Integrated molecular drivers coordinate biological and clinical states in melanoma. *Nat Genet* 2020;52:1373–83.
31 Li J, Liu B, Ye Q, *et al*. Comprehensive genomic analysis of primary malignant melanoma of the esophagus reveals similar genetic patterns compared with epithelium-associated melanomas. *Mod Pathol* 2022;35:1596–608.
32 Lasota J, Kowalik A, Felisiak-Golabek A, *et al*. Primary malignant melanoma of esophagus: clinicopathologic characterization of 20 cases including molecular genetic profiling of 15 tumors. *Mod Pathol* 2019;32:957–66.
33 Sanlorenzo M, Ribero S, Osella Abate S, *et al*. Genetic mutations in primary malignant melanoma of the esophagus: case report and literature review. *G Ital Dermatol Venereol* 2020;155:680–2.
34 Dong Z-Y, Zhong W-Z, Zhang X-C, *et al*. Potential predictive value of TP53 and KRAS mutation status for response to PD-1 blockade immunotherapy in lung adenocarcinoma. *Clin Cancer Res* 2017;23:3012–24.
35 Johnson DB, Lovly CM, Flavin M, *et al*. Impact of NRAS mutations for patients with advanced melanoma treated with immune therapies. *Cancer Immunol Res* 2015;3:288–95.
36 Liu C, Zheng S, Jin R, *et al*. The superior efficacy of anti-PD-1/PD-L1 immunotherapy in KRAS-mutant non-small cell lung cancer that correlates with an inflammatory phenotype and increased immunogenicity. *Cancer Lett* 2020;470:95–105.
37 Devitt B, Liu W, Salemi R, *et al*. Clinical outcome and pathological features associated with NRAS mutation in cutaneous melanoma. *Pigment Cell Melanoma Res* 2011;24:666–72.
38 Zhou L, Wang X, Chi Z, *et al*. Association of NRAS mutation with clinical outcomes of anti-PD-1 monotherapy in advanced melanoma: a pooled analysis of four Asian clinical trials. *Front Immunol* 2021;12:691032.
39 Kirchberger MC, Ugurel S, Mangana J, *et al*. MEK inhibition may increase survival of NRAS-mutated melanoma patients treated with checkpoint blockade: results of a retrospective multicentre analysis of 364 patients. *Eur J Cancer* 2018;98:10–16.
40 Lee JH, Shklovskaya E, Lim SY, *et al*. Transcriptional downregulation of MHC class I and melanoma de- differentiation in resistance to PD-1 inhibition. *Nat Commun* 2020;11:1897.

41 Shklovskaya E, Lee JH, Lim SY, *et al*. Tumor MHC expression guides first-line immunotherapy selection in melanoma. *Cancers* 2020;12:3374.
42 Grasso CS, Tsoi J, Onyshchenko M, *et al*. Conserved interferon-γ signaling drives clinical response to immune checkpoint blockade therapy in melanoma. *Cancer Cell* 2020;38:500–15.
43 Hari L, Miescher I, Shakhova O, *et al*. Temporal control of neural crest lineage generation by Wnt/β-catenin signaling. *Development* 2012;139:2107–17.
44 Dumas LJ, O'Bleness MS, Davis JM, *et al*. DUF1220-domain copy number implicated in human brain-size pathology and evolution. *Am J Hum Genet* 2012;91:444–54.
45 Andries V, Vandepoele K, Staes K, *et al*. NBPF1, a tumor suppressor candidate in neuroblastoma, exerts growth inhibitory effects by inducing a G1 cell cycle arrest. *BMC Cancer* 2015;15:391.
46 Ma R, Jing C, Zhang Y, *et al*. The somatic mutation landscape of Chinese colorectal cancer. *J Cancer* 2020;11:1038–46.
47 Zou Z, Ou Q, Ren Y, *et al*. Distinct genomic traits of acral and mucosal melanomas revealed by targeted mutational profiling. *Pigment Cell Melanoma Res* 2020;33:601–11.
48 Gembarska A, Luciani F, Fedele C, *et al*. MDM4 is a key therapeutic target in cutaneous melanoma. *Nat Med* 2012;18:1239–47.
49 Adhikari H, Counter CM. Interrogating the protein interactomes of RAS isoforms identifies PIP5K1A as a KRAS-specific vulnerability. *Nat Commun* 2018;9:3646.
50 Lionarons DA, Hancock DC, Rana S, *et al*. RAC1^{P29S} induces a mesenchymal phenotypic switch via serum response factor to promote melanoma development and therapy resistance. *Cancer Cell* 2019;36:68–83.